Arab J Geosci (2016) 9: 324
DOI 10.1007/s12517-016-2386-x

ORIGINAL PAPER

# Did satellite imagery supersede aerial imagery? A perspective from 3D geopositioning accuracy

**Altan Yilmaz**[1] · **Mustafa Erdogan**[1] · **Hadi Hakan Maras**[2] · **Bahadir Aktug**[3] · **Suleyman Sirri Maras**[4]

Received: 26 February 2015 / Accepted: 12 February 2016 / Published online: 12 April 2016


**Abstract** In this study, the geometric accuracy comparison of aerial photos and WorldView-2 satellite stereo image data is evaluated with the different number and the distribution of the ground control points (GCPs) on the basis of large scale map production. Also, the current situation of rivalry between airborne and satelliteborne imagery was mentioned. The geometric accuracy of Microsoft UltraCam X 45 cm ground sampling distance (GSD) aerial imagery and WorldView-2 data both with and without GCPs are also separately analyzed. The aerial photos without any GCP by only using global navigation satellite system (GNSS) and inertial measurement unit (IMU) data with tie points give an accuracy of ±1.17 m in planimetry and ±0.71 m in vertical that means nearly two times better accuracy than the rational polynomial coefficient (RPC) of stereo WorldView-2. Using one GCP affects the accuracies of aerial photos and WorldView-2 in different ways. While this situation distorts the aerial photo block, it corrects the shift effect of RPC in WorldView-2 and increases the accuracy. By using four or more GCPs, ½ pixel (~0.23 m) accuracy in aerial photos and 1 pixel (~0.50 m) accuracy in WorldView-2 can be achieved in horizontal. In vertical, aerial photos have 1 pixel (~0.55 m) and WorldView-2 has 1.5 pixels (~0.85 m) accuracy. These results show that Worldview-2 imagery can be used in the production of class I 1:5000 scale maps according to the ASPRS Accuracy Standards for Digital Geospatial Data in terms of geometric accuracy. It is concluded that the rivalry between aerial and satellite imagery will continue for some time in the future.

**Keywords** Aerial photos · WorldView-2 · Geometric correction · Geometric accuracy · Rational functions

✉ Altan Yilmaz
altan.yilmaz@hgk.msb.gov.tr

[1] General Command of Mapping, Ankara, Turkey

[2] Computer Engineering, Cankaya University, Ankara, Turkey

[3] Geophysical Engineering, Ankara University, Ankara, Turkey

[4] Gazi University Polatli Vocational School of Technical Sciences, Ankara, Turkey

## Introduction

The race in space to monitor the earth resources forced the sensors to use digital mediums to store data in spite of films to get rid of the expenses caused by returning the satellite to the Earth (Sandau 2010). This phenomenon brought about the digital sensing. By then, spaceborne sensors have begun to develop in terms of geometric, radiometric, spectral, and temporal resolutions. Parallel to these developments, airborne sensing has made significant improvement since 2000 (Leberl and Gruber 2003). Also by the introduction of fairly large format digital aerial cameras, i.e., UltraCam Eagle by Microsoft and DMC II 250 by Z/I Imaging, it has reached a considerably high level in digital sensing arena (Gruber et al. 2012). So, spaceborne crossed paths with airborne.

The transition from analog aerial film cameras to digital aerial cameras by the emergence of two new cameras, namely ADS-40 by LH-Systems and DMC by Z/I Imaging in 2000, was the milestone of airborne photogrammetry (Leberl and Gruber 2003). With the direct acquisition of imagery, laboratory processing of the analog aerial films has left. Film dispositive and film scanning began to disappear and leave their place to CCD solid-state detectors. So the main error sources in photography were eliminated. It also decreased the personnel and investment costs (Sandau 2010).

The digital aerial cameras enabled users to acquire RGB and NIR data simultaneously in one flight. By the help of

superior radiometry and geometry, digital aerial imagery begun to be used not only for compiling maps but also for remote sensing applications (Sandau 2010).

Relatively small frame sizes of the digital aerial cameras have improved greatly and have reached approximately same level with the analog aerial cameras in the last 3 years with the presentation of UltraCam Eagle by Microsoft and DMC II 250 by Z/I Imaging to the market (Gruber et al. 2012; Jacobsen and Neumann 2012). It is also possible to acquire images with a ground sampling distance (GSD) of 5 cm or better with large format digital aerial cameras.

In order to relate the aerial imagery to the ground, the orientation procedure follows the image acquisition. The orientation of aerial images is calculated by aerial triangulation in aerial photogrammetry (Heipke et al. 2000). Ground control points (GCPs) are needed to calculate the six unknowns (3D coordinates of projection center and the rotation about three axes) of exterior orientation in aerial triangulation. But the boom in technology brought about the global navigation satellite system (GNSS) and inertial measurement unit (IMU) into aerial triangulation providing the elimination or decrease in the number of GCPs. Photogrammetric flights by using GNSS and IMU on board are nearly obligatory today. These systems allow determination of the exterior orientation parameters without using GCPs, and this technique is called direct sensor orientation (Wegman 2002). Before direct sensor orientation, the attitude and shift differences between the IMU and the sensor system (boresight misalignment) have to be determined over a controlled reference area (Jacobsen 2004). The integration of the GNSS/IMU data during the aerial triangulation process provides better approximation values for the automatic procedures. Because of the missing reliability and y-parallaxes during model setup, direct sensor orientation has some disadvantages. These disadvantages can be overcome by a simultaneous adjustment of the directly determined exterior orientation parameters with image coordinates. This method is called integrated sensor orientation (Jacobsen 2004). Especially in wide area mapping projects, integrated sensor orientation can be used to get synergy from classical aerial triangulation and direct sensor orientation (Ip et al. 2007).

On the other hand, remote sensing satellites have acquired data in digital since 1964 (Leberl and Gruber 2003). Three decades after the launch of first civil earth observation satellite Landsat-1 in 1972 with 80-m GSD (Sandau 2010), submeter resolution optic remote sensing satellites have begun to emerge in the market since 1999 with 82-cm resolution IKONOS (Zhou and Li 2000). Since 2007, there have been satellites with GSDs below half a meter, namely Geoeye-1 and WorldView-1/2. Then, the resolution has reached 0.31-cm GSD at nadir by the launch of WorldView-3 to the orbit in 2014 (Satimagingcorp 2015). So far, there were restrictions of US government not to distribute satellite imagery below 50-cm GSD. But this problem was overcome when DigitalGlobe was granted permission from US Department of Commerce to acquire and supply imagery to its customers up to 25-cm GSD in panchromatic and 1.0-m GSD in multispectral (Satimagingcorp 2015).

Due to the different image acquisition structures of the satellites, geometric correction of the satellite imagery is a little bit complicated than the aerial imagery. While aerial cameras take the image at one exposure, generally, optic remote sensing satellites take each individual line at one exposure due to its pushbroom acquisition character (Grodecki and Dial 2003). In order to relate the satellite imagery to the ground, the sensor model of the satellite has to be known. The physical sensor model and the generalized sensor model are widely used imaging geometry models of the remote sensing satellites. The physical sensor model is modeled by the collinearity condition as the aerial photos. The generalized sensor models are the generic models of which parameters do not indicate the physical parameters of imaging (Hu et al. 2004). As described in the ISO 19130 "Geographic information—Imagery sensor models for geopositioning," there are three main replacement sensor models, namely the simple polynomial fitting, ratios of functions (often called the rational functions model—RFM), and the universal real-time model (USM). RFM is the ratio of two polynomials derived from the physical sensor models (Di et al. 2003). The RFM has been widely used in orienting the satellite imagery for nearly two decades due to its capability of providing the full accuracy of different physical sensor models. It is also sensor independent and supplies real-time calculation to approximate the physical sensor models. In this respect, the physical sensor model and the RFM have pros and cons for modeling the satellite imagery. The physical sensor models are generally used to determine the unknown parameters of the RFM for photogrammetric works (Hu et al. 2004).

In order to handle the standard orientation procedures of the satellite imagery, the rational function coefficients (RFCs) of the RFM are provided to the users instead of the physical sensor parameters. This is a good strategy not to hand in the sensor-specific information to the customers to guarantee not to derive the physical sensor parameters from the RFM (Tao and Hu 2002). Because the RFs are the ratios of polynomials, they are also called as rational polynomial coefficients (RPCs).

But the provided RPCs might not yield enough accuracy to compile maps according to some country-specific standards (Di et al. 2003). For example, geolocation accuracy of 46-cm resolution WorldView-2 imagery is below 3.5 m (CE90) without GCPs (14). In order to get the desired accuracy, generally, users prefer to use 2D polynomial functions to correct the ground coordinates derived from the vendor-provided RFCs. At least four GCPs are required to solve a 1st order polynomial, while only one GCP is enough for a 0th order polynomial. This method does not improve RPCs, but only refines coordinates derived directly from the RFCs based on used GCPs (Di et al. 2003). Toutin (2006) attained that with only

using a 0th order polynomial, IKONOS RPC can be refined as well as 1st and 2nd order polynomial functions. On the other hand, he showed that QUICKBIRD RPC can be refined by at least 1st order polynomial. Detailed information for RPC refinement can be found in Di et al. (2003), Tao and Hu (2004), and Zhen and Zhang (2009).

The geometric modeling of these satellites is important, because they can be used to compile and update large scale topographic maps (Poli 2012). According to draft ASPRS Accuracy Standards for Digital Geospatial Data, 40–100-cm GSD is required to fulfill the level of detail for 1:5000 scale maps. Also, 62.5 cm or less $RMSE_x$ (root mean square error) and $RMSE_y$ are the proposed accuracy levels for class I 1:5000 scale maps (ASPRS 2013). In this sense, WorldView-2 satellite imagery seems to fulfill the requirements of large scale maps below or equal to 1:5000. Satellite imagery is the best choice for map production especially for the areas like borders that acquisition of aerial imagery is problematic. There are many studies about the usage of satellite imagery for map production or geometric accuracy of these systems (Li 1998; Zhou and Li 2000; Wang et al. 2005). And generally, these subjects are studied in 2000s. In the last 15 years, there is an important improvement in both airborne and spaceborne imaging systems in terms of resolution, accuracy, quality, and accessibility. Also, there is a doubt among map producers and users about the usage of satellite imagery especially for large scale mapping. Generally, aerial imagery is preferred in map production due to the controlled stages of aerial photography. On the other hand, there are not much studies comparing the aerial and satellite imageries. In this study, the geometric accuracies of the stereo aerial photos and stereo WorldView-2 imagery, which are very important for map production, are investigated with and without GCPs in a test area which reflects the general features of Anatolian peninsula with a focus on the number and the distribution of the GCPs. For the geometric correction of WorldView-2 imagery, similar procedures of aerial imaging like signing of the work area before image acquisition are followed. And they are compared on the 3D geopositioning accuracy basis for large scale map production.

## Study area and data

The study area is situated at the north of Konya, which is a city at the inner part of Anatolia. The area shows the characteristic of much of the inner Anatolia region, with agriculture and urban lands dominating valley bottoms, naked fields and tiny forests covering the steeper areas. The study area is 13.5 km × 16 km, and elevation at the region changes from 1079 to 1961 m. The area is generally rural. At the southeast of the study area, there is Konya Selcuk University Campus, and at the northwest, there is a small village with some agricultural areas. The location of study area in Turkey is shown in Fig. 1. Also, the distribution of GCPs and, independent check points (ICPs) is shown on the height map of the study area in Fig. 2.

Microsoft Vexcel UltraCam X large format digital aerial camera was used to capture 90 images with six strips (four in east-west, two in north-south direction) on 23 April 2010. UltraCam X has 14,430 pixels in cross track and 9420 pixels in flight direction. Its pixel size is 7.2 μm, and focal length is 100.5 mm. The radiometric resolution of the camera is better than 12 bit/channel. The data storage system is able to capture up to 4700 images (Gruber 2008). The aerial photos have 60 % overlap, 30 % sidelap, and 45-cm GSD. The approximate image orientations have been determined by integrated use of GNSS and IMU.

Another image data for the study is stereo WorldView-2 imagery. One of the latest high-resolution satellites, WorldView-2 was launched on 8 October, 2009, joining the Digital Globe Corporate's satellite array consisting of WorldView-1 which was launched in 2007 and QuickBird which was launched in 2001. The high-resolution images provided by the WorldView-2 can be used for a wide range of applications including mapping, disaster relief, defense and intelligence, and classification. WorldView-2 operates at an altitude of 770 km with an inclination angle of 97.2° for a maximum orbital period of 100 min. The satellite has been planned to have a lifespan of 7.5 years. The ability of the satellite to swing rapidly from one target to another allows broad imaging of many targets (Satimagingcorp 2015). Such ability also allows WorldView-2 to collect much more imagery than the total collection capacity of QuickBird and WorldView-1. Another unique characteristic of WorldView-2 is the ability to revisit any place on earth in 1.1 days due to its increased agility and high altitude.

Another advertised quality of WorldView-2 is the advanced geopositional technology which provides a significant improvement in accuracy. The given accuracy specification is 6.5 m CE90 without GCP refinement. Such a high accuracy without any ground control is promising. WorldView-2 also became a commonly used satellite because of its high spatial and spectral resolution and geometric accuracy. Many tests have been carried out to assess the abilities of this system. In a study performed by Cheng and Chaapel (2010), Pan-sharpening and geometric correction of WorldView-2 satellite were tested. Without any GCP, they got an accuracy of 2.6 m in $X$ and 1.3 m in $Y$ with maximum errors of 5.7 m in $X$ and 3.1 m in $Y$. With only one GCP, they achieved an accuracy of 0.7 m in $X$ and 1.0 m in $Y$ with maximum errors of 1.4 m in $X$ and 1.4 m in $Y$. In another study conducted by Deilami and Hashim (2011), very high-resolution optical satellites including WorldView-2 were tested for digital elevation model (DEM) generation.

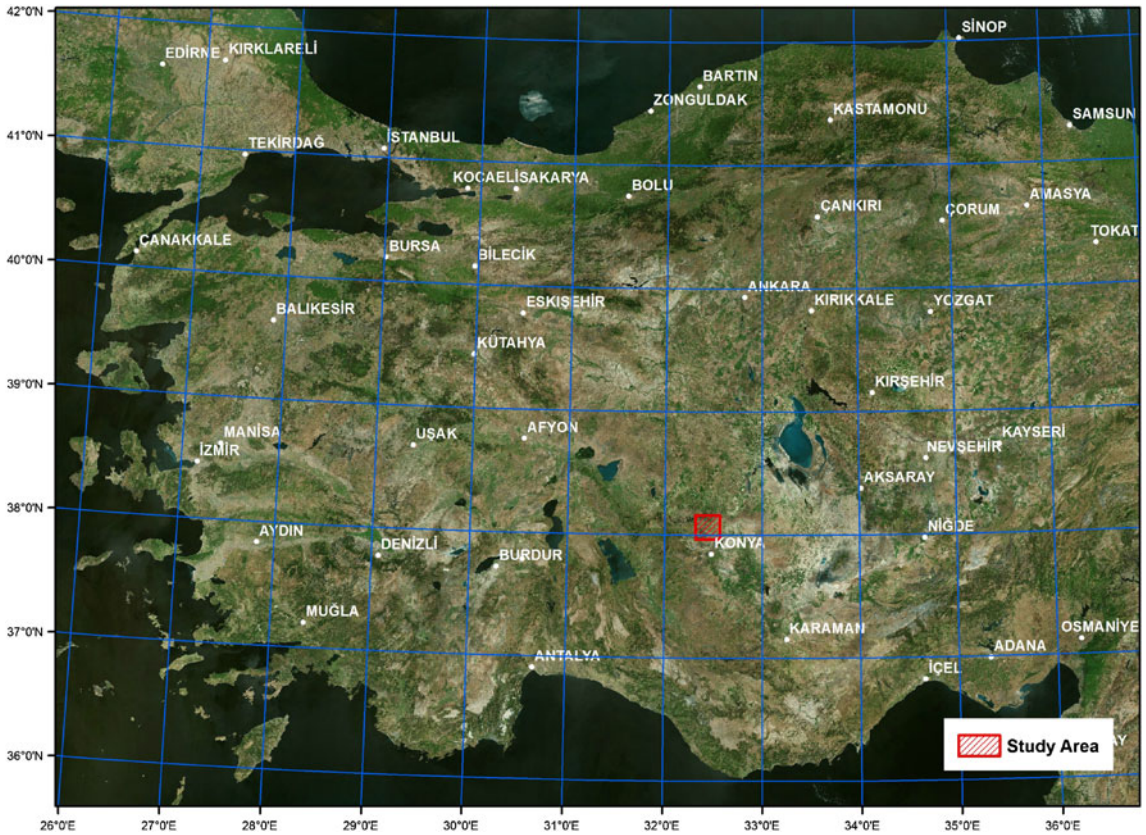


**Fig. 1** Study area

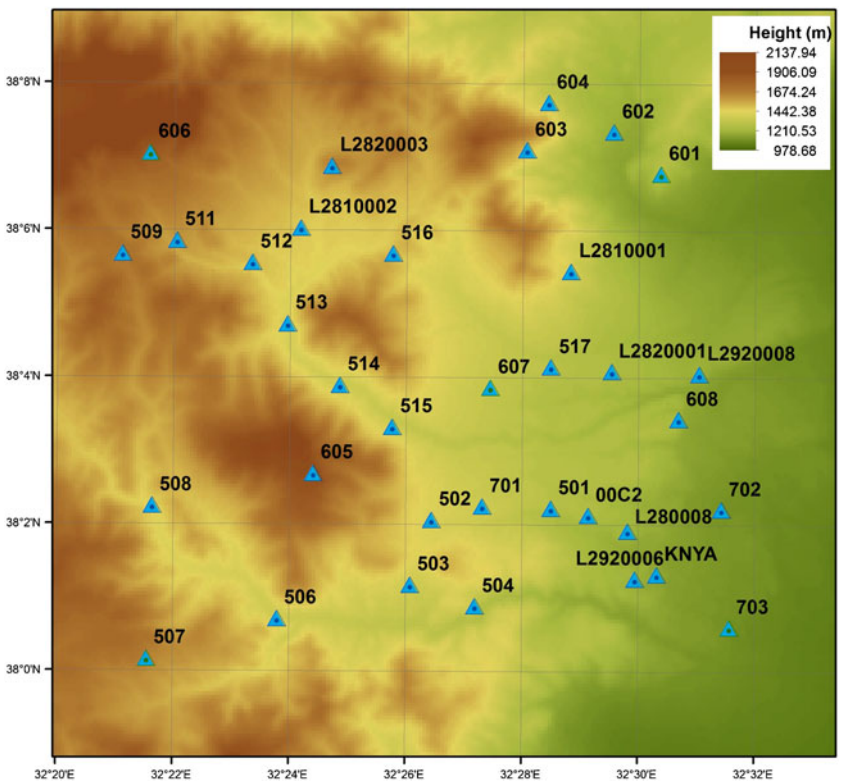


**Fig. 2** GCP and ICP distribution on study area height map

WorldView-2 imagery is supplied by the NIK Company which is the distributer of European Space Imaging GmbH (EUSI) in Turkey. Images are acquired with the approximately 2-min time difference. The images have 16-bit radiometric resolution, and their product level is stereo 2A. Imagery-1 of the stereo pair was acquired by an off-nadir viewing angle of 26° 18′ on 17 June 2010 at 09:02:59Z while Imagery-2 of the stereo pair was acquired by an off-nadir viewing angle of −26° 06′ on 17 June 2010 at 09:04:39Z.

## Field work

Thirty-two ground points are signed and measured before the acquisition of aerial photos and WorldView-2 imagery. Firstly, approximate point locations were chosen over maps with a good horizontal and vertical distribution. After, points were marked by painting on concrete ground or stones, and they were measured by TOPCON HIPer Pro GPS receiver for 1 h. Coordinates of the points were calculated with better than ±5 cm planimetric accuracy (circular error, CE) and ±8 cm vertical accuracy (linear error, LE) by post-processing depending on a constant GPS station.

## Geometric correction of imagery

### Geometric correction of aerial photos

GNSS data are acquired by dual frequency GNSS receivers using differential carrier phase measurements for the aircraft with 1-s interval. A short baseline (i.e., 5 km) between aircraft and reference station is used. The reference station is a station of Turkish National Permanent GNSS Network making observations continuously for 24 h. AeroOffice 5.1 and GrafNav 8.1 software are used for GNSS/IMU process. The boresight misalignment values are set during this process. Images are processed in Microsoft Vexcel UltraMap 3.0 software from level-0 raw data to level-3 pan-sharpened imagery.

Although theoretically it seems possible to calculate the exterior orientation parameters of aerial photos without any control points by only using GNSS/IMU data, aerial triangulation would somewhat be meaningless (Khoshelham 2009). The block would especially have y-parallaxes that will deteriorate stereo map compilation (Ip et al. 2007). The exterior orientation parameters calculated from direct georeferencing will contain systematic drifts and shifts. These projection center coordinates can be refined by using GCPs in aerial triangulation.

GCPs in a block adjustment are generally selected at the corners in order not to extrapolate the projection center coordinates of the aerial photos. Also, using a GCP in block centers may help to detect any deformation. For this reason, aerial block triangulation was run by using different numbers and configurations of GCPs in a rectangular block.

Inpho Match AT 5.4 software is used for automatic aerial triangulation. At first, images' approximate exterior orientation parameters from GNSS/IMU and GCPs are imported in the software. Secondly, image coordinates of GCPs are measured on the images. The control points are defined as GCP or ICP during bundle block adjustment. At first, no GCPs are used, and all the control points are used as ICPs. Only automatically collected tie points and approximate projection center coordinates calculated by GNSS/IMU process are used in bundle adjustment. Secondly, GCP no. 606, GCP no. 601, GCP no. 507, and GCP no. 703 placed on the corners are used as GCP, and all the other points are used as ICPs in four different occasions. Thirdly, GCP no. 607 placed in the middle of the block is used as GCP, and all the other points are used as ICPs. Fourthly, GCP nos. 606 and 703, GCP nos. 601 and 507 placed on the cross corners are used as GCPs, and all the other points are used as ICPs in two different occasions. Fifthly, GCP nos. 606, 601, 703, and 507 placed on the cross corners are used as GCPs, and all the other points are used as ICPs. Lastly, GCP nos. 606, 601, 507, and 703 placed on the corners and 607 placed in the middle are used as GCPs, and all the other points are used as ICPs. For self-calibration, 12 parameters are selected in the software. The bundle adjustment is performed for each situation according to the number and distribution of control points. The results are presented in Table 1. "*S*" is the horizontal RMSE in Table 1.

As seen in Table 1, it can be said that no or only one GCP may be enough for aerial triangulation when using GNNS and IMU accompanying with aerial imagery. It can be seen in Table 1 that by using no GCP may yield as good accuracy as one GCP in planimetry while it is nearly 2.5 times worse in height. It is due to the nature of GNSS. If only planimetric coordinates are of importance, using no GCP will be a good choice. But, using GCPs at least in the block corners are needed to accurately define GNSS corrections. In case one GCP is used, the block accuracy will be susceptible to the quality of IMU data and GCP itself. The drift and shift effects cannot be modeled properly by using only one GCP. Getting far away from a GCP will produce larger residuals theoretically. If one GCP is used in aerial triangulation, the center of the block will be the best location due to its distance to the whole block. In case of no GCP, ICPs should be used in the center of the block in order to define the deformation. Using GCPs in the block corners will yield a much reasonable error distribution by spreading errors throughout the whole block.

### Geometric correction of WorldView-2 imagery

Leica Photogrammetry Suite (LPS) software 9.2 version is used in the geometric correction of WorlView-2 imagery. Firstly, the project is defined, and rational functions as

**Table 1** Aerial triangulation results

| Distribution of the GCP | ICP/GCP no. | Control point RMSE (m) | | | | Check point RMSE (m) | | | |
|---|---|---|---|---|---|---|---|---|---|
| | | *X* | *Y* | *S* | *Z* | *X* | *Y* | *S* | *Z* |
| No GCP | 28/0 | | | | | 0.964 | 1.044 | 1.421 | 2.423 |
| At the corner (no. 606) | 27/1 | | | | | 1.161 | 1.673 | 2.036 | 1.067 |
| At the corner (no. 601) | 27/1 | | | | | 1.037 | 1.264 | 1.635 | 0.580 |
| At the corner (no. 507) | 27/1 | | | | | 1.519 | 1.492 | 2.129 | 1.350 |
| At the corner (no. 703) | 27/1 | | | | | 1.250 | 1.642 | 2.064 | 0.697 |
| In the middle (no. 607) | 27/1 | | | | | 0.983 | 1.031 | 1.425 | 1.069 |
| Cross corners (nos. 606, 703) | 27/2 | | | | | 0.138 | 0.174 | 0.222 | 0.602 |
| Cross corners (nos. 601, 507) | 27/3 | | | | | 0.160 | 0.190 | 0.248 | 0.577 |
| At the corners (nos. 606, 703, (nos. 601, 507) | 24/4 | 0.044 | 0.060 | 0.074 | 0.209 | 0.174 | 0.156 | 0.234 | 0.634 |
| At the corners and in the middle (nos. 606, 703, (nos. 601, 507, 607) | 23/5 | 0.044 | 0.055 | 0.070 | 0.218 | 0.159 | 0.163 | 0.228 | 0.496 |

geometric model category and WorldView rational polynomial coefficient (RPC) as geometric model are selected.

Two different approaches are followed at the block measurements. At the first approach, all 32 points are used as GCP or ICP that means the sum of numbers of GCPs and ICPs is always 32. At the beginning, 25 points were measured as GCP and the other 7 as ICP. Later, the number of GCPs is decreased, and the remaining control points were used as ICP. At the second approach, again, all 32 points are used as GCP or ICP at the beginning (25 GCPs and 7 ICPs). Later, the number of GCPs is decreased but the number and distribution of ICPs were kept constant and same 7 ICPs were used for the accuracy assessment of different numbers and distributions of GCPs. Also, in both approach, 1st or 0th order polynomial corrections were tested. The satellite orbits are very stable and smooth, so high degrees of polynomials are not preferred. When the higher polynomial degrees are used, the number of needed GCPs increases and geometry may be distorted with inadequate GCPs. For this reason, generally, 1st or 0th order polynomial corrections are used for the geometric correction of satellite imagery with RPC model. Especially to see the effect of GCP position, when the only one GCP is used, this point is selected both in the middle and corner of the images.

Also, 63 tie points were measured. The imagery block is triangulated with different GCP/ICP numbers and distributions, and polynomial orders and accuracies are calculated. The results are given in Table 2. It can be seen from Table 2 that even the use of one GCP supplies very good accuracy. In all GCP numbers and distributions, accuracies in *X* and *Y* directions are nearly 1 pixel or better. The number of GCPs and polynomial order especially affects the accuracy in *Z*. When more GCPs are used, 1st order polynomials achieve higher accuracy in *Z*. But adversely when the less GCPs are used, 0th order polynomials achieve higher accuracy in *Z*. Use of more than nine GCPs does not affect the overall accuracy remarkably in any direction. When one GCP is used, points selected at the corners decrease the accuracy and a point in the middle should be preferred.

## The comparison of geometric accuracies

The comparison of geometric accuracies of the aerial photos and WorldView-2 imagery is shown in Table 3. In Table 3, similar GCP distributions are compared at the same row. The graphic representations of the accuracies are given in Fig. 3.

The results show that aerial photos have generally two times better accuracies than WorldView-2 imagery without any GCPs or with two or more GCP cases. Only in one GCP case, WorldView-2 gives better results. Use of more than one GCP remarkably changes the accuracy of aerial imagery. For WorldView-2, the use of GCP affects the accuracy, but change according to the number of GCPs is not very clear and regular as aerial imagery.

Subpixel accuracy in horizontal can be accomplished for aerial photographs by using two or more GCPs. For WorldView-2 imagery, generally, an accuracy of 1 pixel can be reached by using one or more GCPs. In vertical, both types of imagery give an accuracy of 2 pixels.

By using no GCP, WorldView-2 gives ellipsoid height due to the nature of RPC. By using 0th order 2D polynomial, the ellipsoid height can be shifted to orthometric height. For both systems, at least one GCP should be used to get orthometric heights or generated height may be corrected with an appropriate geoid model.

For WorldView-2 imagery, 1st order polynomials give slightly better results when high number of GCPs is used. But when GCP number is decreased nearly fewer than 10, 0th order polynomial gives better results. These results can

**Table 2** WorldView-2 triangulation results

| GCP/ICP no. | Approach no. | Poly. order | Control point RMSE (m) | | | | Check point RMSE (m) | | | |
|---|---|---|---|---|---|---|---|---|---|---|
| | | | *X* | *Y* | s | *Z* | *X* | *Y* | s | *Z* |
| 25/7 | 1 and 2 | 1 | 0.190 | 0.248 | 0.312 | 0.745 | 0.230 | 0.294 | 0.373 | 0.754 |
| | | 0 | 0.215 | 0.260 | 0.337 | 0.825 | 0.208 | 0.312 | 0.375 | 0.863 |
| 17/15 | 1 | 1 | 0.225 | 0.263 | 0.346 | 0.832 | 0.194 | 0.254 | 0.320 | 0.671 |
| | | 0 | 0.258 | 0.275 | 0.377 | 0.875 | 0.169 | 0.280 | 0.327 | 0.785 |
| 17/7 | 2 | 0 | 0.258 | 0.275 | 0.377 | 0.875 | 0.208 | 0.339 | 0.398 | 0.810 |
| 13/19 | 1 | 1 | 0.267 | 0.230 | 0.352 | 0.750 | 0.221 | 0.287 | 0.362 | 0.740 |
| | | 0 | 0.297 | 0.259 | 0.394 | 0.842 | 0.181 | 0.289 | 0.341 | 0.832 |
| 13/7 | 2 | 0 | 0.297 | 0.259 | 0.394 | 0.842 | 0.236 | 0.298 | 0.380 | 0.843 |
| 11/21 | 1 | 1 | 0.283 | 0.245 | 0.374 | 0.693 | 0.210 | 0.273 | 0.344 | 0.795 |
| | | 0 | 0.315 | 0.276 | 0.419 | 0.755 | 0.167 | 0.276 | 0.323 | 0.871 |
| 11/7 | 2 | 0 | 0.315 | 0.276 | 0.419 | 0.755 | 0.228 | 0.301 | 0.378 | 0.847 |
| 9/23 | 1 | 1 | 0.337 | 0.278 | 0.437 | 0.669 | 0.283 | 0.256 | 0.382 | 0.956 |
| | | 0 | 0.312 | 0.312 | 0.441 | 0.813 | 0.257 | 0.257 | 0.363 | 0.855 |
| 9/7 | 2 | 0 | 0.312 | 0.312 | 0.441 | 0.813 | 0.282 | 0.306 | 0.416 | 0.842 |
| 5/27 | 1 | 1 | 0.038 | 0.231 | 0.234 | 0.600 | 0.231 | 0.400 | 0.462 | 1.028 |
| | | 0 | 0.218 | 0.238 | 0.323 | 0.846 | 0.230 | 0.410 | 0.470 | 0.833 |
| 5/7 | 2 | 0 | 0.218 | 0.238 | 0.323 | 0.846 | 0.187 | 0.509 | 0.542 | 0.868 |
| 4/28 | 1 | 1 | 0.040 | 0.123 | 0.129 | 0.163 | 0.225 | 0.491 | 0.540 | 1.135 |
| | | 0 | 0.239 | 0.131 | 0.273 | 0.713 | 0.234 | 0.498 | 0.550 | 0.874 |
| 4/7 | 2 | 0 | 0.239 | 0.131 | 0.273 | 0.713 | 0.194 | 0.598 | 0.629 | 0.844 |
| 3/29 | 1 | 1 | 0.025 | 0.007 | 0.026 | 0.007 | 0.230 | 0.353 | 0.421 | 1.031 |
| | | 0 | 0.155 | 0.334 | 0.368 | 0.522 | 0.269 | 0.337 | 0.431 | 0.868 |
| 3/7 | 2 | 0 | 0.164 | 0.161 | 0.230 | 0.691 | 0.264 | 0.543 | 0.604 | 0.842 |
| 2/30 | 1 | 0 | 0.266 | 0.013 | 0.266 | 0.689 | 0.342 | 0.354 | 0.492 | 1.033 |
| 2/7 | 2 | 0 | 0.106 | 0.071 | 0.128 | 0.336 | 0.298 | 0.291 | 0.417 | 0.909 |
| 1/31 (corner) | 1 | 0 | 0.000 | 0.000 | 0.000 | 0.000 | 0.231 | 0.510 | 0.560 | 1.391 |
| 1/31 (middle) | 1 | 0 | 0.000 | 0.000 | 0.000 | 0.000 | 0.230 | 0.277 | 0.360 | 1.134 |
| 1/7 (corner) | 2 | 0 | 0.000 | 0.000 | 0.000 | 0.000 | 0.167 | 0.286 | 0.331 | 1.570 |
| 1/7 (middle) | 2 | 0 | 0.000 | 0.000 | 0.000 | 0.000 | 0.162 | 0.270 | 0.315 | 1.412 |
| 0/32 (3D) | 1 | 0 | 0.000 | 0.000 | 0.000 | 0.000 | 1.881 | 1.345 | 2.312 | 2.540 |
| 0/32 (2D) | 1 | 0 | 0.000 | 0.000 | 0.000 | 0.000 | 1.877 | 1.346 | 2.310 | 0.000 |
| 0/7 (3D) | 2 | 0 | 0.000 | 0.000 | 0.000 | 0.000 | 1.889 | 1.213 | 2.245 | 2.550 |
| 0/7 (2D) | 2 | 0 | 0.000 | 0.000 | 0.000 | 0.000 | 1.889 | 1.213 | 2.245 | 0.000 |

be explained with the higher number of unknowns of the 1st order polynomial that should be solved. The affect of using higher order of polynomials and breaking points according to the number of GCPs can be tested in a region having more GCPs in further studies.

## Results

In this study, aerial photographs and WorldView-2 imagery are geometrically corrected with different numbers and distributions of GCPs, and accuracies are investigated by ICPs.

For aerial photos, the geolocation error using only GNSS, IMU data, and also automatically collected tie points without any GCPs is less than 1 m in *X*, *Y*, and *Z* directions, which are a very good result, can be used in many applications. It is possible to use GCPs to correct the errors in the GNSS and IMU data. But using only one GCP, the accuracy is subject to pointing and measuring of that point. Especially using one GCP at the corner may distort the block and may decrease the accuracy. Using four or more GCPs which is an ideal block configuration increases the accuracy to approximately 1/3 pixel size in *X* and *Y* directions and 1 pixel size in *Z* direction. Using GNSS during image

**Table 3** The comparison of geometric accuracies

| Distribution of the GCP | GCP no. | Aerial photos RMSE (m) | | | | WorldView-2 RMSE (m) | | | |
|---|---|---|---|---|---|---|---|---|---|
| | | x | y | s | z | x | y | s | z |
| No GCP | 0 | 0.964 | 1.044 | 1.421 | 2.423 | 1.881 | 1.345 | 2.312 | 2.540 |
| In the middle | 1 | 0.983 | 1.031 | 1.425 | 1.069 | 0.230 | 0.277 | 0.360 | 1.134 |
| Cross corners | 2 | 0.138 | 0.174 | 0.222 | 0.602 | 0.342 | 0.354 | 0.492 | 1.033 |
| Cross corners | 3 | 0.160 | 0.190 | 0.248 | 0.577 | 0.230 | 0.353 | 0.421 | 1.031 |
| At the corners | 4 | 0.174 | 0.156 | 0.234 | 0.634 | 0.234 | 0.498 | 0.550 | 0.874 |
| At the corners and in the middle | 5 | 0.159 | 0.163 | 0.228 | 0.496 | 0.230 | 0.410 | 0.470 | 0.833 |

acquisition provides better approximation for defining exterior orientation parameters for automatic tie point collection. Adding IMU data makes the direct georeferencing possible by providing directly the exterior orientation parameters. But, there still exists some systematic errors that have to be corrected. The systematic errors (GNSS drifts and shifts) can be detected and eliminated by a suitable GCP distribution over the block. In case of direct georeferencing, ICPs should be used in the center of the block in order to define the deformation. Using GCPs in the cross corners will yield as good accuracy as block corners. But in order to stay on the safe side, for a reasonable error distribution throughout the whole block and overcome any deformation of the block, it is recommended to use four GCPs on the block corners and one more in the middle of the block.

For WorldView-2 imagery, the geolocation error using only supplied RPCs without any GCPs is less than 2 m in both *X* and *Y* directions. It is possible to use GCPs to correct the errors in the supplied RPCs and thus improving the geolocation accuracy. Even the use of only one accurate GCP increases the accuracy nearly to 0.5-m level. The total horizontal RMSEs change between 0.320 and 0.629 m, and vertical RMSEs change between 0.671 and 1.570 m by using one or more GCPs. Use of more than ten GCPs does not affect accuracy level significantly. The affect polynomial order of the geometric correction is also tested. Generally, the use of 0th order polynomials is enough, and 1st order polynomials only change the accuracy 1 to 2 cm. Hence, 0th order polynomial refinement to the RPC model can be used for geometric modeling of WorldView-2 data. GCP distribution affects the accuracy 5 to 20 cm since the measurement of some GCP image coordinates may not be very precise. Similar geolocation accuracies with different GCP distributions can be expected with better quality image measurement. For further studies, tests may be conducted in wider areas with large terrain variations.

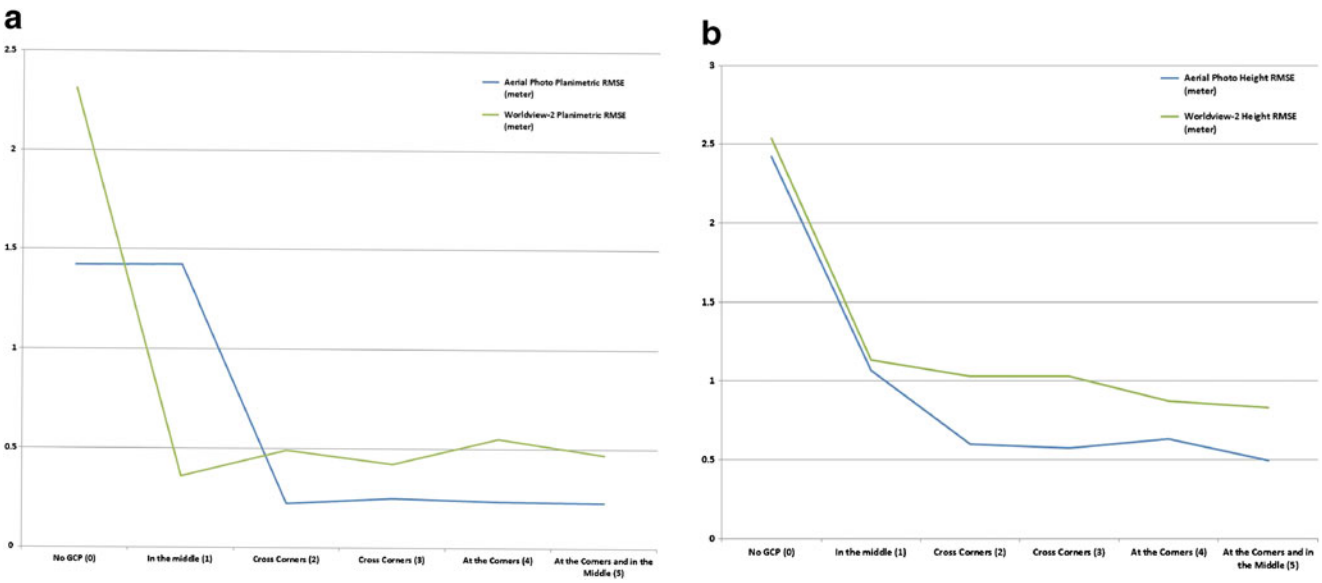


**Fig. 3** Geometric accuracies. **a** Planimetric. **b** Height

## Conclusion

This paper compares the geometric accuracies of the aerial photos and WorldView-2 data having similar GSD with different GCP numbers and distributions by means of ICPs.

GCP RMSE used in geometric correction reveals internal accuracy, in other words, modeling accuracy and GCP measurement/marking accuracy on the ground and imagery. On the other hand, ICP RMSE shows outer accuracy, meaning, geopositioning accuracy of the features on Earth (Toutin 2004).

Unless using any GCP, GNSS and IMU data together with tie points for aerial photos yield two times better accuracy than the RPC modeling of stereo WorldView-2. Using one GCP affects the accuracies of aerial photos and WorldView-2 in different ways. While this situation distorts the aerial photo block, it corrects the shift effect of RPC on WorldView-2 and increases the accuracy. By using four or more GCPs, ½ pixel accuracy in aerial photos and 1 pixel accuracy in WorldView-2 can be obtained in horizontal plane. Also by using four or more GCPs, 1 pixel accuracy in aerial photos and 1.5 pixel accuracy in WorldView-2 can be obtained in vertical.

WorldView-2 fulfills requirements for draft ASPRS Accuracy Standards for Digital Geospatial Data of 1:5000 scale topographic maps. It is also allowed but not recommended being used in even larger scales, i.e., 1:2500.

Both image sources can be used in many applications. But, especially in applications requiring higher accuracy and a stable block, aerial photos may be preferred. Especially for scales larger than 1:5000, the use of aerial photography is recommended. Also, it should be taken into consideration that the control point requirement for WorldView-2 in wide areas will be higher in order to maintain similar accuracies with aerial photos. In urgent situations and unreachable areas, WorldView-2 or similar high-resolution satellite imagery will be a good choice for users.

However, the satellite imagery is so close to aerial imagery in 3D geometric geopositioning accuracy, and it has not superseded aerial imagery yet. It seems that the rivalry will continue for some time in the future.

## References


ASPRS (2013) ASPRS accuracy standards for digital geospatial data (draft for review). Photogramm Eng Remote Sens 79(12): 1073–1085

Cheng P, Chaapel C (2010) Pan-sharpening and geometric correction of WorldView-2 satellite. GEOInformatics 2010:30–33

Deilami K, Hashim M (2011) Very high resolution optical satellites for Dem generation: a review. Eur J Sci Res 49(4):542–554

Di K, Ma R, Li R (2003) Rational functions and potential for rigorous sensor model recovery. Photogramm Eng Remote Sens 69(1):33–41

Grodecki J, Dial G (2003) Block adjustment of high-resolution satellite images described by rational functions. Photogramm Eng Remote Sens 69:59–69

Gruber M (2008) UltraCamX, the new digital aerial camera system by Microsoft Photogrammetry. The International Archives of the Photogrammetry, Remote Sensing and Spatial Information Sciences XXXVII-B1:665–670

Gruber M, Ponticelli M, Ladstadter R, Wiechert A (2012) Ultracam Eagle, details and insight. International Archives of the Photogrammetry, Remote Sensing and Spatial Information Sciences XXXIX-B1:15–19

Heipke C, Jacobsen K, Wegmann H (2000) Integrated sensor orientation—an OEEPE Test. International Archives of Photogrammetry and Remote Sensing XXXIII-B3:373–380

Hu Y, Tao V, Croitoru A (2004) Understanding the rational function model: methods and applications. International Archives of Photogrammetry and Remote Sensing XXXV-B4:663–668

Ip A, El-Sheimy N, Mostafa M (2007) Performance analysis of integrated sensor orientation. Photogramm Eng Remote Sens 73(1):1–9

Jacobsen K (2004) Direct integrated sensor orientation—pros and cons. The International Archives of the Photogrammetry, Remote Sensing and Spatial Information Sciences XXXV-B3:829–835

Jacobsen K, Neumann (2012) Property of the large format digital aerial camera DMC II. International Archives of the Photogrammetry, Remote Sensing and Spatial Information Sciences XXXIX-B1:21–25

Khoshelham K (2009) Role of tie points in integrated sensor orientation for photogrammetric map compilation. Photogramm Eng Remote Sens 75(3):305–311

Leberl F, Gruber M (2003) Flying the new large format digital aerial camera UltraCam-D. Photogrammetric Week 2003, D. Fritsch, Ed. Wichmann-Verlag, Heidelberg: 67–76

Li R (1998) Potential of high-resolution satellite imagery for national mapping products. Photogramm Eng Remote Sens 64:1165–1170

Poli D (2012) Review of developments in geometric modelling for high resolution satellite pushbroom sensors. Photogramm Rec 27(137): 58–73

Sandau R (2010) Digital airborne camera: introduction and technology. Springer Science and Business Media. doi:10.1007/978-1-4020-8878-0

Satimagingcorp (2015) WorldView-2 satellite sensor, http://www.satimagingcorp.com/satellite-sensors/worldview-2/. Accessed on 26 Feb 2015

Tao V, Hu Y (2002) 3D Reconstruction methods based on the rational function model. Photogramm. Eng Remote Sens 68(7):705–714

Tao V, Hu Y (2004) RFM: an open sensor model for cross sensor mapping. ASPRS Conference 23–28 May, Denver, 9 p

Toutin T (2004) GCP requirement for high resolution satellite mapping. The International Archives of the Photogrammetry, Remote Sensing and Spatial Information Sciences XXXV-B3:836–839

Toutin T (2006) Comparison of 3D physical and empirical models for generating DSMs from stereo HR images. Photogramm Eng Remote Sens 72(5):597–604

Wang J, Di K, Li R (2005) Evaluation and improvement of geopositioning accuracy of IKONOS stereo imagery. J Surv Eng 131(2):35–42

Wegman H (2002) Image orientation by combined (A)AT with GPS and IMU. Proceeding of ISPRS Commission I Symposium http://www.isprs.org/proceedings/XXXVII/congress/2_pdf/6_WG-II-6/12.pdf. Accessed on 26 Feb 2015

Zhen X, Zhang Y (2009) A generic method for RPC refinement using ground control information. Photogramm Eng Remote Sens 75(9): 1083–1092

Zhou G, Li R (2000) Accuracy evaluation of ground points from IKONOS high-resolution satellite imagery. Photogramm Eng Remote Sens 66(9):1103–1112